

# Symmetry-conserving vortex clusters in small rotating clouds of ultracold bosons

Igor Romanovsky, Constantine Yannouleas, and Uzi Landman  
*School of Physics, Georgia Institute of Technology, Atlanta, Georgia 30332-0430*  
 (Dated: 21 February 2008; Physical Review A **78**, 011606 (2008), Rapid Communication)

The properties of a special class of correlated many-body wave functions, named rotating vortex clusters (RVCs), that preserve the total angular momentum of a small cloud of trapped rotating bosons are investigated. They have lower energy and provide a superior description for the formation of vortices compared to the mean-field Gross-Pitaevskii (GP) states that break the rotational symmetry. The GP vortex states are shown to be wave packets composed of such RVC states. Our results suggest that, for a small number of bosons, the physics is different from that of ideal Bose-Einstein condensates which characterize larger assemblies.

PACS numbers: 03.75.Hh, 03.75.Lm, 03.75.Nt

Mean-field descriptions of the many-body problem exhibit a ubiquitous symmetry-breaking behavior that extends across several fields of physics, from nuclear physics [1], quantum chemistry [2], and metallic microclusters [3] to semiconductor quantum dots [4] and trapped ultracold atoms [4, 5, 6].

Mean-field broken-symmetry solutions are expected to play the role of an effective ground state in the thermodynamic limit,  $N \rightarrow \infty$ , when quantum fluctuations about the mean-field state may be omitted [7]. A prominent example of such broken-symmetry states is given by the Gross-Pitaevskii (GP) vortex states in a harmonic trap [8]. Specifically, although each individual vortex carries a quantized amount of angular momentum [9], the GP vortex solutions as a whole break the rotational symmetry of the confining harmonic trap [10], and thus they are not eigenstates of the total angular momentum  $\hat{L} = \sum_{i=1}^N \hat{l}_i$ . In agreement with the general ideas of Ref. [7], GP vortex states have been observed experimentally (see, e.g., Refs. [11, 12, 13, 14]) for rotating Bose gases with large  $N$ . Indeed the energy advantage of symmetry restored states (see below) over the mean-field solutions diminishes as  $N$  increases (see section 1.2. in Ref. [4]).

Recently, the availability of optical lattices [15, 16] with a small number of particles per lattice site serves to motivate studies of small clouds of rotating bosons. For a small number  $N$  of atoms, however, quantum fluctuations cannot be neglected, and one needs to consider methods beyond the mean-field approximation [4].

A natural way for accounting for quantum correlations about the GP vortex solutions in a harmonic trap is the method of restoration of rotational symmetry via projection techniques. This method [4] was introduced recently in quantum dots [17, 18] and harmonic traps [5, 19] to describe *individual particle localization* and formation of rotating electron molecules (REMs) [20] and rotating boson molecules (RBMs), respectively. Here, we use projection techniques to define and study vortex states with *good* total angular momentum, showing that these states can be properly referred to as rotating vortex clusters (RVCs). We stress again that the RVCs are eigenstates

of the total angular momentum in contrast to the GP vortex states. For small  $N$ , the rotating-vortex-cluster states are the natural entities to be employed (in place of the GP vortices) for comparisons with exact solutions, which are eigenstates of the total angular momentum by their very nature. Furthermore we note the generality of the methodology of symmetry restoration. It applies as well to other broken symmetries, like spin symmetries [4].

We derive the RVC wave function by using an adaptation of the two-step many-body method of symmetry breaking/symmetry restoration. We start with the observation that the *many-body* GP vortex solution,  $\Psi^{\text{GP}}$ , (as well as any mean-field solution exhibiting a breaking of the rotational symmetry) is a wave packet, and thus it can be expanded as a linear superposition over eigenstates  $\Phi_{N,L}$  of the many-body Hamiltonian  $\mathcal{H}$  with good total angular momentum  $L$ , i.e.,

$$\Psi_N^{\text{GP}}(\mathbf{r}_1, \mathbf{r}_2, \dots, \mathbf{r}_N) = \sum_L C_L \Phi_{N,L}(\mathbf{r}_1, \mathbf{r}_2, \dots, \mathbf{r}_N). \quad (1)$$

For the two-dimensional case considered here (which is appropriate for a rapidly rotating harmonic trap), the eigenstates  $\Phi_{N,L}$ 's can be approximated by using the projection operator

$$\hat{\mathcal{P}}_L = \frac{1}{2\pi} \int_0^{2\pi} d\theta e^{i\theta(L-\hat{L})} = \delta(L - \hat{L}), \quad (2)$$

which projects states with good total  $L$  out of the GP vortex state. The RVC wave functions are then given by

$$|\Phi_{N,L}^{\text{RVC}}\rangle = \hat{\mathcal{P}}_L |\Psi_N^{\text{GP}}\rangle = \int_0^{2\pi} d\theta |\Psi_N^{\text{GP}}(\theta)\rangle e^{i\theta L}, \quad (3)$$

where  $|\Psi_N^{\text{GP}}(\theta)\rangle$  is the original many-body GP vortex solution rotated by an azimuthal angle  $\theta$ . The projection techniques use the fact that the broken-rotational-symmetry states form a manifold of energy degenerate states (i.e., their total energy is independent of the azimuthal angle  $\theta$ ); in this respect, the phases  $e^{i\theta L}$  in Eq.

(3) are the characters of the rotational group in two dimensions.

The expansion coefficients  $C_L$  in Eq. (1), which specify the spectral decomposition of the many-body Gross-Pitaevskii vortex state, can be calculated using the projected wave functions (3) for the  $\Phi_{N,L}$ 's in the r.h.s of Eq. (1). Taking into consideration that  $\Psi_N^{\text{GP}}(\mathbf{r}_1, \mathbf{r}_2, \dots, \mathbf{r}_N) = \prod_{i=1}^N \phi_0(\mathbf{r}_i)$ , one finds

$$C_L = \frac{1}{2\pi} \int_0^{2\pi} d\theta n(\theta) e^{i\theta L}, \quad (4)$$

where the overlap kernel is given by  $n(\theta) = \langle \phi_0(\theta=0) | \phi_0(\theta) \rangle^N$ , and the multiply occupied orbital  $\phi_0(\mathbf{r})$  is a solution of the familiar Gross-Pitaevskii equation

$$[H(\mathbf{r}) + g(N-1)|\phi_0(\mathbf{r})|^2]\phi_0(\mathbf{r}) = \varepsilon_0 \phi_0(\mathbf{r}), \quad (5)$$

with the single-particle Hamiltonian given by  $H(\mathbf{r}) = \mathbf{p}^2/(2m) - \Omega \hat{l} + m\omega_0^2 \mathbf{r}^2/2$ , where  $\Omega$  is the rotational frequency of the trap and  $\omega_0$  characterizes the circular harmonic confinement.

The total energy of the RVC is given by

$$E_{N,L}^{\text{RVC}} = \int_0^{2\pi} h(\theta) e^{i\theta L} d\theta / \int_0^{2\pi} n(\theta) e^{i\theta L} d\theta, \quad (6)$$

with the Hamiltonian kernel being  $h(\theta) = \langle \Psi_N^{\text{GP}}(\theta=0) | \mathcal{H} | \Psi_N^{\text{GP}}(\theta) \rangle$ , where the many-body Hamiltonian is  $\mathcal{H} = \sum_{i=1}^N H(\mathbf{r}_i) + g \sum_{i<j}^N \delta(\mathbf{r}_i - \mathbf{r}_j)$ . The above constitutes an effective continuous configuration-interaction scheme which lowers the mean-field energy by introducing correlations [4]. The lowering of the ground-state energy brought about by the angular-momentum projection can be seen (see Ref. [21]) from evaluation of the GP ground-state energy using the spectral decomposition given in Eq. (1). This yields the expression  $E_N^{\text{GP}} = \sum_L |C_L|^2 E_{N,L}^{\text{RVC}}$  with  $\sum_L |C_L|^2 = 1$ . Since  $E_N^{\text{GP}}$  is expressed as a weighted average of  $E_{N,L}^{\text{RVC}}$  with positive weights, it is obvious that at least one of these energies obeys  $E_{N,L}^{\text{RVC}} \leq E_N^{\text{GP}}$ .

To illustrate the essential qualitative difference between the RVCs and the GP vortex states, we contrast in Fig. 1 their single-particle densities (SPDs) for the case of  $N = 9$  trapped bosons and when the GP solutions exhibit either a (0,4) single-polygonal-ring of four [Fig. 1(a)] or a (2, 5) double-polygonal-ring configuration of seven [Fig. 1(b)] localized vortices (for the trap and other parameters employed, see the caption of Fig. 1);  $(n_1, n_2)$  denotes  $n_1$  ( $n_2$ ) vortices on the inner (outer) ring. In sharp contrast to the GP single-particle densities, the RVC SPDs are circularly symmetric: the one [Fig. 1(c)] corresponding (through the aforementioned projection) to the four GP vortices exhibits instead a single continuous ring of depleted matter, while the other one [Fig.

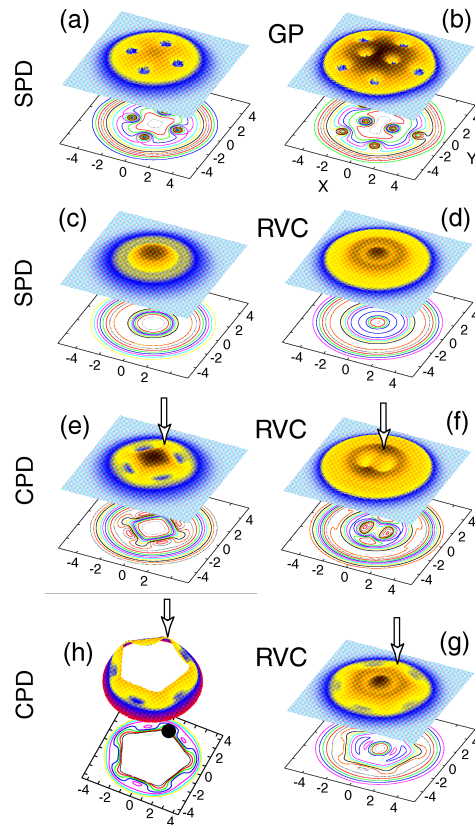


FIG. 1: Rotating vortex cluster and GP vortex solutions for  $N = 9$  trapped bosons in a rotating trap with angular frequencies of trap rotation  $\Omega/\omega_0 = 0.5$  [top three panels in the left column] and  $\Omega/\omega_0 = 0.565$  [all four panels in the right column plus (h)]. For  $\Omega/\omega_0 = 0.5$ , a (0,4) single-polygonal ring of four vortices is involved, while for  $\Omega/\omega_0 = 0.565$  a (2,5) double-polygonal ring of seven vortices develops. (a,b) GP single-particle densities (SPDs). (c,d) RVC single-particle densities. (e-h) RVC conditional probability distributions (CPDs), with the fixed point (marked by a thick vertical arrow) at  $\mathbf{r}_0 = (0, 2.07l_0)$  (e),  $\mathbf{r}_0 = (0, 1.14l_0)$  (f), and  $\mathbf{r}_0 = (0, 3.2l_0)$  (g,h). (h) A horizontal slice of the CPD in (g) which magnifies the five vortices of the outer ring. The RVC total angular momenta are  $L = 28$  [(c) and (e)] and  $L = 36$  [(d),(f-h)]. The corresponding GP total-angular-momentum averages ( $\langle \Psi_N^{\text{GP}} | \hat{L} | \Psi_N^{\text{GP}} \rangle$ ) are 26.93 and 38.11, respectively. Note the elliptic shape of the vortex cores in the CPDs [see (e-h)] reflecting azimuthal fluctuations in the RVC state. The strength of the interparticle repulsion was taken  $R_\delta = 50$  [ $R_\delta \equiv gm/(2\pi\hbar^2)$ , see Ref. [5]]. Unit length:  $l_0 = \sqrt{\hbar/(m\omega_0)}$ .

1(d)] corresponding to the seven GP vortices exhibits instead two concentric continuous rings of depleted matter.

Due to the symmetry restoration, the vortex structures become “hidden” in the RVC single-particle densities. However, they can be revealed through the use of conditional probability distributions (CPDs) defined as

$$P(\mathbf{r}, \mathbf{r}_0) = \langle \Phi_{N,L}^{\text{RVC}} | \sum_{i \neq j} \delta(\mathbf{r}_i - \mathbf{r}) \delta(\mathbf{r}_j - \mathbf{r}_0) | \Phi_{N,L}^{\text{RVC}} \rangle. \quad (7)$$

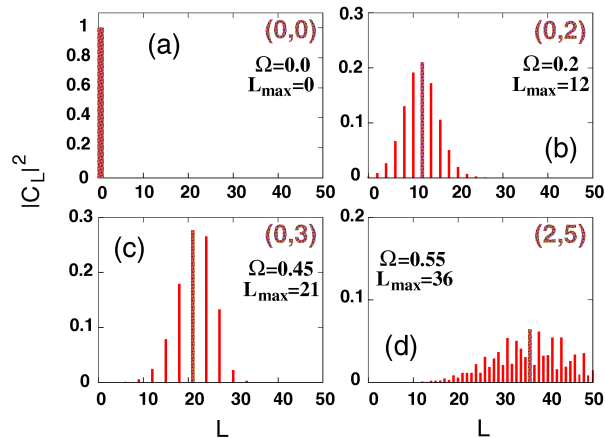


FIG. 2: Spectral decomposition [ $C_L$  coefficients modulus square, Eq. (4)] for GP vortex ground states in characteristic cases. Angular frequency of the trap: (a)  $\Omega/\omega_0 = 0$ . (b)  $\Omega/\omega_0 = 0.2$ . (c)  $\Omega/\omega_0 = 0.45$ . (d)  $\Omega/\omega_0 = 0.55$ . The total angular momenta associated with the largest coefficients are  $L_{max} = 0, 12, 21$ , and  $36$ , respectively. The polygonal ring configurations of the GP vortices are also marked as  $(n_1, n_2)$ . The ratio of the interparticle repulsion and the kinetic energy was taken  $R_\delta = 50$  (see caption of Fig. 1). In the figure,  $\Omega$  is given in units of  $\omega_0$ . The GP total-angular-momentum expectation values are (a)  $0.0$ , (b)  $11.01$ , (c)  $21.42$ , and (d)  $36.53$ .

CPDs give the probability of finding a boson at position  $\mathbf{r}$  given that another boson is located at a fixed point  $\mathbf{r}_0$ .

In the CPDs calculated for the RVC states [see Figs. 1(e,f,g,h)], the fixed point is associated with a hump (local maximum) and the vortices are given by depressions (local minima) in the matter density. The number of vortices of a GP state and of an RVC projected out from it is the same for all  $\Omega$ 's; e.g., in the CPD in Fig. 1(e) four vortices are seen corresponding to the four GP vortices in Fig. 1(a). This reflects the fact that the projection maintains the same (intrinsic or hidden) point-group symmetry.

For the  $(2, 5)$  double-ring RVC, the fixed point can be placed on the inner or the outer ring. In the first case, the calculated CPD [Fig. 1(f)] shows two vortices on the inner ring and remains uniform along the outer ring, while in the second case the calculated CPD [Fig. 1(g,h)] shows five vortices on the outer ring and remains uniform along the inner ring. This suggests that the rings rotate independently of each other in analogy with the case of rotating boson molecules [19] and rotating electron molecules in quantum dots [4].

To further investigate the wave-packet properties of the GP vortices, we have numerically calculated their spectral decomposition in terms of RVC states [see Eq. (1)]. In Fig. 2, we plot the expansion coefficients  $C_L$  [calculated numerically according to Eq. (4)] for  $N = 9$  bosons and for several characteristic angular frequencies. The

$\Omega = 0$  case is a rather trivial one where the GP solution preserves the circular symmetry, exhibits no vortices, and coincides with the corresponding RVC for  $L = 0$  (in this limiting case, one has  $C_0 = 1$  and  $C_L = 0$  for any  $L \neq 0$ ).

For the chosen value  $R_\delta = 50$  (see the caption of Fig. 1), non-trivial cases arise for  $\Omega/\omega_0 > 0.175$ . For  $\Omega/\omega_0 = 0.2$  [Fig. 2(b)] and  $\Omega/\omega_0 = 0.45$  [Fig. 2(c)] the GP vortex solutions exhibit a  $(0,2)$  and  $(0,3)$  single polygonal-ring configurations, respectively. The expansion coefficients  $C_L$  clearly demonstrate that the GP vortex states given as examples in these figures can be reconstructed from linear superpositions of RVC states [observe the many non-vanishing values of  $C_L$  in Fig. 2(b) and Fig. 2(c)]. Of central importance is the selection rules that the RVC angular momenta must obey in order to be compatible with the  $(n_1, n_2)$  intrinsic RVC point-group symmetry (which coincides with the explicit point-group symmetry of the associated GP vortex states). Indeed, for the  $(0,2)$  vortex ring the RVC angular momenta obey the relation  $L = 2k$ , while for the  $(0,3)$  case, one has  $L = 3k$ , with  $k = 0, 1, 2, \dots$ . The RVC angular momenta vary in a stepwise manner, and the value of the step coincides with the number of GP vortices on the single ring. For  $\Omega/\omega_0 = 0.55$ , the GP vortex state exhibits a double  $(2,5)$  polygonal-ring structure, which imposes upon the RVC decomposition a more complex, but approximate, selection rule  $L = 2k_1 + 5k_2$ , with both  $k_1$  and  $k_2$  being positive integer numbers. While the larger  $C_L$ 's [Fig. 2(d)] conform to this rule, there are several smaller  $C_L$ 's whose angular momenta fall outside this rule. The reason is that in the GP solution [see Fig. 1(b)] the arrangement of vortices on the outer ring deviates slightly from being a perfect regular pentagon [22].

From the many RVC states that contribute at a given  $\Omega$  to the spectral decomposition of the GP vortex states (including in the latter both ground and low-lying excited configurations), there is one with lowest energy  $E_{GS}^{RVC}$ , which is the ground state within the RVC approximation at this specific rotational frequency. For the  $\Omega$ 's and the parameters considered in Fig. 2, we found that the RVC ground states have angular momenta  $L_{GS}$  associated with the largest coefficients  $|C_L|$  in the GP decompositions; these  $L_{GS}$ 's always obey the polygonal-ring selection rules discussed above.

As aforementioned from the general theory of projection techniques [21], the RVC ground-state energies are lower than (or equal at most to) the corresponding GP ones for all values of the rotational frequency (Fig. 3). Furthermore, the angular momenta associated with the RVC ground states are quantized and thus exhibit a stepwise increase as a function of the rotational frequency (see Fig. 4). The magnitude of the steps in the ground-state RVC angular momenta changes with  $\Omega$ , since RVCs with different  $(n_1, n_2)$  intrinsic vortex configurations become the ground-state as  $\Omega$  increases. This behavior contrasts with that of the ground-state GP angular momenta

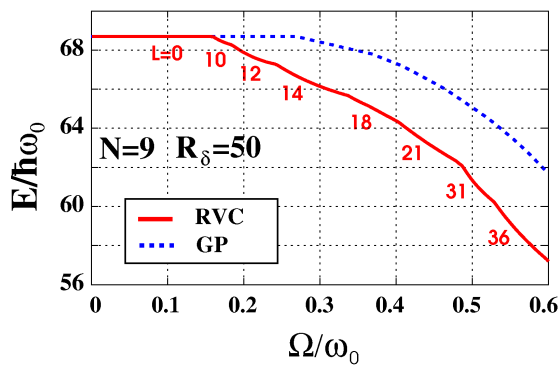


FIG. 3: RVC (solid) and GP (dotted) ground-state energies for  $N = 9$  bosons and  $R_\delta = 50$ , plotted versus the rotational frequency  $\Omega/\omega_0$ . The ground-state angular momenta are denoted under the RVC curve.

that vary continuously as a function of  $\Omega$  without any direct association to the  $(n_1, n_2)$  vortex configuration (Fig. 4). In several instances, the RVC ground state has an intrinsic  $(n_1, n_2)$  point-group symmetry that is different from that of the GP vortex ground state at the same  $\Omega$ . This happens when the projection of an excited GP state results in a larger energy gain compared with that of the GP ground state.

While we focus here on obtaining a proper symmetry-conserving vortex theory for a finite (small) number of trapped bosons, we comment on the RVC behavior compared with that obtained through exact diagonalization (EXD) calculations, which have become in recent years computationally feasible for smaller  $N$ . In particular, unlike the RVC case studied here (see Fig. 4), EXD calculations in the lowest Landau level for  $N = 9$  bosons exhibit quantized ground-state “magic” angular momenta that follow a  $L_m = n_1 k_1 + n_2 k_2$  selection rule, but with the additional condition  $n_1 + n_2 = N$  (unlike the RVC behavior where  $n_1 + n_2 = q \neq N$ ); see, e.g., Fig. 10 in Ref. [23] and Fig. 2 in Ref. [24]. Moreover, it was shown in Ref. [23] that EXD ground-state wave functions describe formation of a rotating boson molecule [5, 19] exhibiting two distinct (1,8) and (2,7) isomers of localized bosons.

The above characteristic difference between the RVC and RBM [19, 23] solutions maintains for other values of  $N$  and  $R_\delta$ , reflecting the intrinsic point group symmetry of the angular momentum conserving theory (RVC, RBM via projection methods [19] or EXD [23]). This is particularly the case for low  $N$  and high  $R_\delta$ , where the RBMs are energetically favored and the RVCs may be regarded as higher lying excited states. However, for higher  $N$  (occurring earlier for low  $R_\delta$ ) the RVC may compete effectively with the localized RBM states, and eventually become the ground state.

In conclusion, we have introduced a correlated many-body wave function, referred to as a rotating vortex cluster, which conserves the total angular momentum and

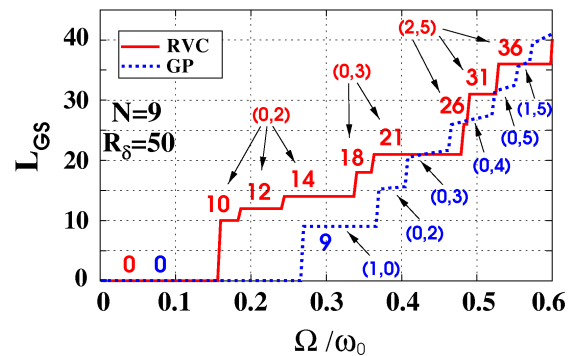


FIG. 4: RVC (solid) and GP (dotted) ground-state angular momenta for  $N = 9$  bosons and  $R_\delta = 50$ , plotted versus the rotational frequency  $\Omega/\omega_0$ . The quantized RVC angular momenta are explicitly denoted in the figure, along with the corresponding polygonal-ring configurations  $(n_1, n_2)$ . The Gross-Pitaevskii  $(n_1, n_2)$  configurations are also denoted. The GP angular momenta are not quantized; they are given by the expectation values  $\langle \Psi_N^{\text{GP}} | \hat{L} | \Psi_N^{\text{GP}} \rangle$ .

has lower energy compared to the Gross-Pitaevskii solution. The RVC is better suited to describe formation of vortices in small rotating clouds of trapped bosons compared to the mean-field GP vortex states that break the rotational symmetry. The GP vortex states were shown to be wave packets composed of such RVC states. The calculation of the properties of rotating-vortex-cluster states allowed for comparisons of qualitative signatures (e.g., ground-state angular momenta sequences) between the RVC and exact-diagonalization results. We conclude that the physics of small rotating bosonic clouds is markedly different from that of larger assemblies known to behave as ideal Bose-Einstein condensates (properly described by the broken symmetry GP vortex solutions). We hope that these results will motivate further experimental research in the area of correlated states in small bosonic systems (see, e.g., Ref. [25]).

This work was supported by the US D.O.E. (Grant No. FG05-86ER45234).

- 
- [1] P. Ring and P. Schuck, *The Nuclear Many-body Problem* (Springer-Verlag, New York, 1980).
  - [2] R. Carbó and M. Klobukowski, *Self-Consistent Field: Theory and Applications* (Elsevier, Amsterdam, 1990).
  - [3] C. Yannouleas *et al.*, In *Metal Clusters*, edited by W. Ekardt (Wiley, Chichester, 1999), p. 145.
  - [4] C. Yannouleas and U. Landman, *Rep. Prog. Phys.* **70**, 2067 (2007).
  - [5] I. Romanonsky *et al.*, *Phys. Rev. Lett.* **93**, 230405 (2004).
  - [6] E.J. Mueller *et al.*, *Phys. Rev. A* **74** 033612 (2006).
  - [7] P.W. Anderson, *Basic Notions of Condensed Matter Physics* (Addison-Wesley, Reading, MA, 1984), pp 44 - 47.
  - [8] L.P. Pitaevskii and S. Stringari, *Bose-Einstein Condensates*

- sation (Oxford: Oxford University Press, Oxford, 2003).
- [9] G. Baym, *J. Low Temp. Phys.* **138**, 601 (2005).
  - [10] R.A. Butts and D.S. Rokhsar, *Nature (London)* **397**, 327 (1999).
  - [11] K.W. Madison *et al.*, *Phys. Rev. Lett.* **84**, 806 (2000).
  - [12] C. Raman *et al.*, *Phys. Rev. Lett.* **87**, 210402 (2001).
  - [13] P.C. Haljan *et al.*, *Phys. Rev. Lett.* **87**, 210403 (2001).
  - [14] E. Hodby *et al.*, *Phys. Rev. Lett.* **88**, 010405 (2002).
  - [15] M. Greiner *et al.*, *Nature (London)* **415**, 39 (2002).
  - [16] M. Lewenstein *et al.*, *Advances in Physics* **56**, 243 (2007).
  - [17] C. Yannouleas and U. Landman, *J. Phys.: Condens. Matter* **14**, L591 (2002).
  - [18] C. Yannouleas and U. Landman, *Phys. Rev. B* **66**, 115315 (2002).
  - [19] I. Romanovsky *et al.*, *Phys. Rev. Lett.* **97**, 090401 (2006).
  - [20] Another term is rotating Wigner molecules (RWMs).
  - [21] P.-O. Löwdin, *Rev. Mod. Phys.* **34**, 520 (1962).
  - [22] The five GP vortices [Fig. 1(b)] are located at different distances from the center at  $3.29l_0$ ,  $2.78l_0$ ,  $2.96l_0$ ,  $2.96l_0$ , and  $2.78l_0$  (the azimuthal angles between neighboring vortices also deviate slightly from the ideal value of  $2\pi/5$ ). This originates from intervortex repulsion.
  - [23] L.O. Baksmaty *et al.*, *Phys. Rev. A* **75**, 023620 (2007).
  - [24] N. Barberan *et al.*, *Phys. Rev. A* **73**, 063623 (2006).
  - [25] N.D. Gemelke, Ph.D. Dissertation (Stanford University, 2007); Steven Chu, Book of Abstracts, *International Conference on Atomic Physics 2008*, p. 5; N.D. Gemelke, E. Sarajlic, and S. Chu, *ibid.*, p. 363.